EXPLOITING CARBON NANOTUBE NETWORKS FOR DAMAGE ASSESSMENT OF STRUCTURAL COMPOSITES

A. Baltopoulos[a], N.Polydorides[b], L.Pambaguian[c], A. Vavouliotis[a], V. Kostopoulos*[a]

[a]*Applied Mechanics Laboratory, Department of Mechanical Engineering and Aeronautics, University of Patras, GR26504, Greece*
[b]*Institute for Digital Communications, School of Engineering, The University of Edinburgh, Edinburgh, United Kingdom*
[c]*Materials and Components Technology Division, European Space Agency (ESA/ESTEC), Noordwijk, The Netherlands*
**kostopoulos@mech.upatras.gr*

Keywords: carbon nanotubes, fibre reinforced plastics, electrical tomography, non-destructive testing.

Abstract

A novel approach for damage inspection of composite structures utilizing carbon nanotubes (CNT) networks is investigated. CNT are dispersed in an epoxy using a high shear mixing technique and subsequently used as matrix for a structural glass fiber reinforced plastic (GFRP). Damage interrupts the continuity of the CNT network separating and isolating regions of the conductive network. Employing electric potential fields these changes can be measurable and can provide information on the location of the damage. Electrical Resistance Tomography (ERT) is presented and experimentally applied to measure changes in the potential fields and deliver electrical conductivity change maps which are used to identify and locate changes in the CNT networks. These maps are correlated to damage in the composite. The technique shows sensitivity to very small damages; less than 0.1% of the inspected area. The solution of the inverse ERT problem delivers conductivity change maps, for different damage modes, which offers an effective localization with nearly 10% error and an inspection area suppression around 75%.

1. Introduction

Damage assessment of composite materials and structures is becoming increasingly important as a consequence of their increased use in a variety of applications, such as energy and aerospace. Various Non-Destructive Evaluation (NDE) techniques are available to detect damage in composites with the most commonly employed being ultrasonic (e.g. C-scan), thermography etc. Acoustic emission, fiber Bragg gratings and use of vibrational methods have attracted a great amount of attention the past years. In parallel, the progress in nanotechnology has enabled the development of novel materials routes for developing multi-functional material systems and structures that incorporate approaches for damage detection.

Products of nanotechnology, such as Carbon Nanotube (CNT) or other nanoparticles have been proposed as enablers of mechanical performance enhancement of composites [1]. Promising results have been reported in fatigue, fracture and post impact performance of such systems [2]. Further to the mechanical performance though, CNT networks developed within polymer matrices have been investigated for damage sensing and monitoring in a number of studies as a means towards multifunctional material systems. Most of the works are based on the Electrical Resistance Change Method (ERCM) where the apparent macroscopic resistance of the conductive network is monitored. Relation has been proven between the recorded electrical resistance change and the incidents and/or the mechanical degradation of the material. Studies have covered a wide spectrum of materials; nanocomposite polymers [3] and polymer foams [4], GFRP [5-8], CFRP [9]. Finite Element (FE)

models have also been employed to verify the experimental findings [10]. It can be said that electrical-based methods, such as ERCM, offer the potential of a tool for sensing the development and evolution of damage as well as health monitoring of conductive composite structures.

In order for both CNT networks and electrical based methods to reach real structural applications at large scale, further developments in the direction to cover the localization and size of the damage need to take place, based on the needs of practice. A number of studies have worked in extending electrical sensing principles to 2D using electrical conductivity mapping [11], electric potential fields [12] or other approaches [13]. A brief summary of the ideas is presented in [14]. Limited works have been reported in the direction of exploiting nanoparticle networks in structural composites to provide 2D inspection information [15-19]. Alternative routes based on nanotechnology and multi-physics fields have also been proposed by Guzman de Villoria et al [20] enabling good spatial resolution for sensing damage in composites.

In the present work, we develop a CNT network within the matrix of a, formerly, non-conductive fibrous composite and exploit it, not only to sense the damage state, but to provide information on where damage is located. This work bridges the field between the research by Proper et al [17] and Hou et al [18]. We use polymer processing techniques compatible with composite manufacturing techniques to develop a CNT network within the matrix of a structural composite and take a step further from the state-of-the-art in sensing studies utilizing CNT networks, by providing a structured methodology to calculate inspection maps useful for locating damage in structural composite parts. For this to happen, Electrical Resistance Tomography (ERT) [11, 21] is used as a methodology to collect and process the experimental recordings borrowing experience from other scientific fields [22, 23]. The result of ERT inverse problem solution is a map of expected conductivity change where one can identify regions of interest and thus serve as a tool for the NDE of composite parts. It is believed that the proposed approach is scalable and can serve as the basis for further applications of CNT networks in real structures.

2. Principle idea of the work

The CNT reinforced GFRP essentially comprises a three-phase composite system. Both glass fibers and the matrix material are insulating phases. The only path for charge transport in the composite is the conductive CNT network. The network extends throughout the matrix of the composite providing an efficient path for electron flow, similar to distributed network of resistors [24]. As in previously mentioned studies, this inherent conductivity of the composite is used for NDE. The principle idea of this work is illustrated in a simplified way in the schematic of Figure 1. For clarity, glass fibers are excluded from the schematic.

Injecting a current at different ends of the CNT network stimulates different regions of the network and develops a different voltage distribution throughout the material. Thus, as it seems natural, when monitoring the voltage at the same end of the network a different voltage value will be recorded (Figure 1-a, b). Maximizing the sensitivity of the voltage measurement by adjusting the current injection point seems like a logical approach. When damage is considered, any defect in the CNT network (e.g. due to cracking or delamination or example) will create a local disruption of the electrical network (Figure 1-c, d). Parts of the network may be separated and isolated and this will have an effect on the total apparent resistance (seen by the current source) and the local current flow (seen at the voltage measurement ends). This means that when injecting a current at the same location to the network, a different electrical potential field will be established between the undamaged and the damaged state. Taking a step further, by injecting current at different points of the network, the effect of the disturbance on the boundary voltage measurements may be magnified or suppressed.

These two observations form the basis of the proposed tomographic technique. Based on a vector of electrical potential information measured at the boundary of the composite laminate, we attempt to inversely calculate the conductivity distribution change within the material. Because the CNT are

considered homogeneously distributed within the matrix in a 3D configuration, this enables a global monitoring of the composite laminate and can address various related damage modes.

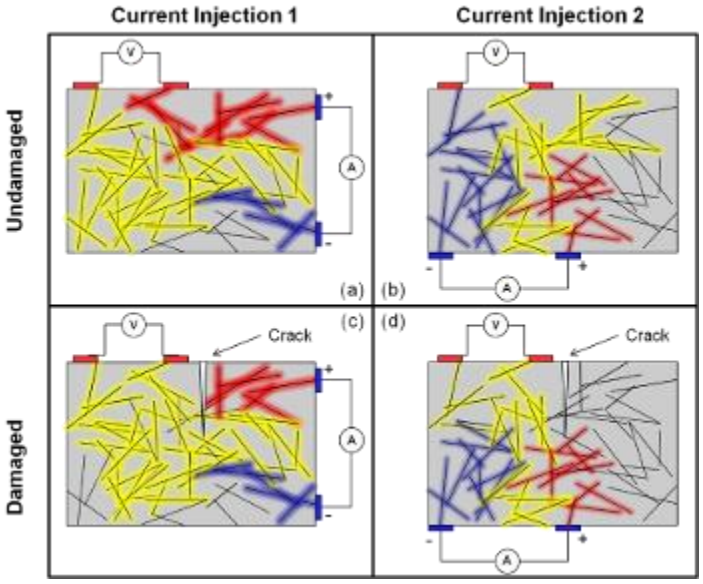

Figure 1. CNT network and Principle of ET technique; (Red: High voltage, Yellow: Medium voltage, Blue: Low voltage).

3. Materials, Methods and Experimental Approach

3.1. Preparation of CNT/Epoxy mixture and manufacturing of composite material

Epoxy resin L1100 (with Hardener 295) commercially available by R&G Composite Technologies GmbH (Germany) was used as the host matrix. It is a low viscosity resin system, widely used in wind turbine blade manufacturing. The macro-scale reinforcing phase was a glass fiber twill woven fabric having a 163gr/m^2 area weight also procured by R&G Composite Technologies GmbH (Germany). MWCNT produced by catalyzed CVD were supplied by ARKEMA (France) in raw powder form. The MWCNT had a diameter ranging from 10 to 15nm and length more than 500nm, resulting in an aspect ratio between 30 and 50. Preparation and dispersion procedures used in previous studies [6, 25] utilizing the same batch of CNT showed good mechanical and electrical results for polymer composites. Therefore the same procedures were followed and the CNT were used as received, i.e. no treatment or functionalization took place. Any humidity present was eliminated by placing the CNT in an oven at 60^{o}C overnight, prior to the mixing process.

The dispersion and composite manufacturing procedure is shown in Figure 2. The first step is to disperse the MWCNT in Part-A of the epoxy system (Step 1). High-shear mixing dissolver device by VMA Getzmann GmbH (Germany) was used to homogeneously disperse the CNT within Part A of the epoxy system. A rotating disk introduces shear forces to the mixture creating a vortex flow, which leads to a continuous mixing of the compound. The shear forces disentangle the CNT and reduce their agglomerates. The dissolver disc rotational speed was 2500rpm and the mixing duration was 3hrs. The temperature was controlled between 40-50^{o}C using a water cooled double walled container. The mixing was done under vacuum to avoid any air inclusion. The technique has proven to be effective in dispersing CNT in epoxy systems in order to produce electrically conductive composites, utilizing efficiently the advantage of high aspect ratio of the CNT [25].

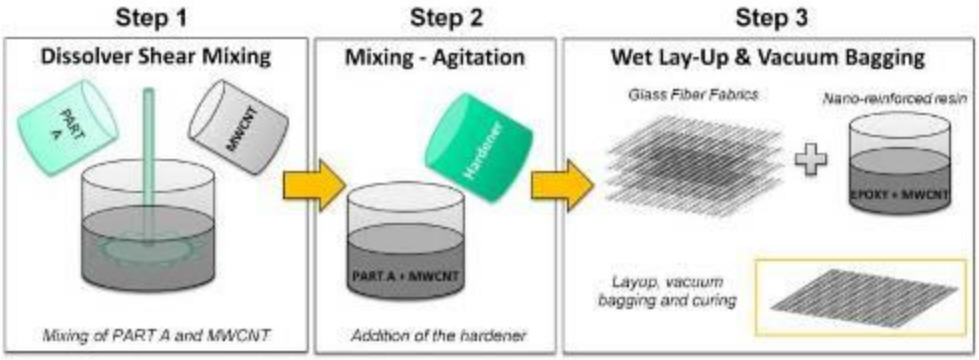

Figure 2. Preparation of CNT reinforced polymer and GFRP plate.

Then the hardener was added (Step 2) and subsequently the nano-reinforced resin was used to fabricate glass fiber composites (Step 3). Prior to layup the resin was degassed for 15min. Twelve (12) layers having the same orientation were used. Wet-layup technique followed by vacuum bagging was used. The lay-up took place on a rigid flat aluminum mould. Once the wet lay-up process was finished, the stack was hermetically enclosed in a vacuum bag and put in an oven to cure for 6hrs at 50^{o}C. The produced plate had a thickness of 2.5mm. The targeted CNT concentration in the final composite was 0.5%wt. The resulting volume fraction of the composite was determined to be in the range of 47%. Square 100mm specimens were cut from the plate using a diamond-grit circular disk. The specimens were prepared for ERT by positioning 20 peripheral electrodes close to the edge of the plate. Firstly, a 1mm diameter hole is drilled at the desired point. The inner surface of the hole is painted with conductive silver-paint to provide a good interface and minimize contact resistance with the circular cross section copper electrode, which is placed tightly into the hole. A two part conductive epoxy is used to hold the electrode cables in place (similar to [18, 21]). The epoxy was cured for 4hrs at 55^{o}C.

3.2. Material Characterization

Scanning Electron Micrographs were used to evaluate the dispersion of CNT within the matrix. Images were taken using LEO SUPRA 35VP at various magnification levels for a set of random samples from the material. Complementing SEM observations, electrical conductivity was used as another indicator of the achieved CNT dispersion. A KEITHLEY 2002 digital multimeter by Keithley Instruments Inc. (USA) was used for the electrical measurements. Measurements were made in three directions corresponding to the three principle axes of the material. This was done under the scope of verifying that the architecture of the layup did not induce any anisotropic electrical behavior. Specimens were cut from the manufactured plate; oblong specimens 100x15mm for in-plane measurements [26] and square 25x25mm specimens for the through thickness direction. The electrode contact surfaces were sanded to smooth the roughness and then silver painted.

3.3. Damage modes assessed

To assess the sensing capabilities of ERT on these materials, three different scenarios were evaluated in this study; a through-thickness hole, an oblong notch and indentation damage. The hole is the first/baseling damage implemented to assess the capabilities of NDE/SHM methods. Here a small hole having a diameter of 3mm was made to the plate. The damage corresponds to less than 0.1% of the total area of the composite plate being inspected. An oblong notch is another typical damage mode and is an approach to assess the capability of the technique to detect cracks. An oblong crack (length = 12mm, t=2mm) was created using a cutting disc and a high speed rotary tool (DREMEL). The damage region represented nearly 0.2% of the total inspected area. Finally, Quasi-Static Indentation (QSI) testing was employed to experimentally assess BVID resembling damage. In QSI, a hemispherical indenter is pushed against a simply supported specimen. The support is a circular ring (0.05m diameter) leaving the space under the specimen right below the indentation point free to deform. To assess the developed damage and for direct evaluation of the ERT results, ultrasonic inspection (C-scan) was employed.

3.4. ERT theory, post-processing and application

The forward electrical problem is to derive the voltage distribution given the conductivity distribution within a medium and the current injection input. Mathematically this is done by solving Equation 1 in the conductive medium Ω, given respective appropriate boundary conditions:

$$\nabla \cdot (\sigma \nabla u) = 0 \ , \qquad \bar{r} \in \Omega \tag{1}$$

Where σ is the conductivity distribution and u is the electrostatic potential.

ERT is the process of approximating the conductivity distribution of the interior of a body from the knowledge of injected currents and measured voltages at its surface (referred as the Electrical Tomography Inverse Problem (ETIP)). A series of electrodes is placed at the periphery of the part under inspection. Current is injected through a selected set of electrodes and voltage measurements are recorded on the rest of them. The process is organized in a protocol which defines which electrodes are active (current bearing) and which are passive (voltage sensing). The recorded measurements along with the geometry of the component and electrode location are used as input for the inverse calculation of the conductivity change distribution. Certain sets of electrodes for current injection may prove more informative and can provide greater amount of information, based on the type, the location and the extent of damage. However, since the damage characteristics are unknown, there is no a-priori knowledge.

ETIP is an ill-posed problem and intrinsically non-linear which means that small variations in the input (voltage measurements) may have large effects on the output (conductivity maps). This nature of inverse ERT problems sets limitations to the capabilities of the technique. Ill-posed problems and techniques to address this issue are discussed in depth in [22, 27]. To deal with the ill-posedness of the inverse problem, we employ a post-processing scheme recently proven to perform well in materials of similar nature [21]. The mathematical inversion of the experimental data to calculate the conductivity change map is performed following the Tikhonov regularization (Equation 2) [23]:

$$d\sigma_{Tikhonov} = \min(\|dV - J(d\sigma)\|^2 + \lambda \|L \cdot d\sigma\|^2) \tag{2}$$

Where: $d\sigma_{Tikhonov}$ is the conductivity change vector, dV is the experimentally recorded voltage change between two states, J is the Jacobian mapping the conductivity change to voltage change on the electrodes, λ is the regularization parameter and L is the regularization matrix. Essentially, it is a Least Squares approach augmented by an additional penalty to large solutions. Regularization improves the conditioning of the problem, enabling a numerical solution. The identity matrix was used as L to avoid any bias to the solution, while a heuristic approach was followed to select the value of λ.

For the solution of Equation 2, a FE scheme is employed in the mathematical formulation of the inverse problem [27, 28]. The conductivity is kept constant within each element of the FE mesh, while the voltage was piecewise linear. The process essentially assigns a conductivity change value to each element of the mesh to reach a best fit solution of J(dσ) to dV which is governed by the Jacobian of the inverse problem (J). The outcome is an electrical conductivity change map depicting where changes are expected between the two states compared; an increase in the conductivity change map is essentially a region where conductivity is expected to drop.

As a step to further automate the damage assessment and to enhance the localization of the technique, two indices are calculated for each calculated map; the Centre of Interest (CoI) and the respective Region of Interests (RoI). The former refers to the mathematical areal weighted mean of the conductivity change distribution while the later is the 1-σ region around the CoI.

For implementing experimentally the technique, an ERT system was developed. A conceptual illustration of the ERT system and the process as applied in this work is shown in Figure 4-a. The experimental setup used in this work is shown in Figure 4-b. The ERT system consists of a programmable DC source (KEITHLEY 224) and a data acquisition switch board unit with an internal digital multi-meter (AGILENT 34970A). Dedicated routines control the switching within the cards of the data acquisition unit to deliver the current at the desired electrodes and take the voltage measurements according to a specified protocol.

The opposite current injection protocol [27] for collecting the voltages is used. A total of 10 current patterns is used. Each current pattern (20 measurements each sub-set). This results in signature with a global set of 200 measurements. The protocol runs as follows. Current is injected between the first pair of electrodes (electrodes 1 & 11 – current pattern 1-11). A sub-set of voltage measurements is taken for all the electrodes with reference to the ground (V@1,2,3,...,20). Then, the next current pattern is applied at the next opposite electrode pair (current pattern 2-12). Again the system is allowed to settle and the respective sub-set of voltage measurements (V@1,...,20) is recorded. This loop is continued for current patterns up to 10-20 where the process is ended. A signature set is taken prior to damage as reference and another signature set is recorded after the damage is introduced. Their difference is the input (dV) for Equation 2.

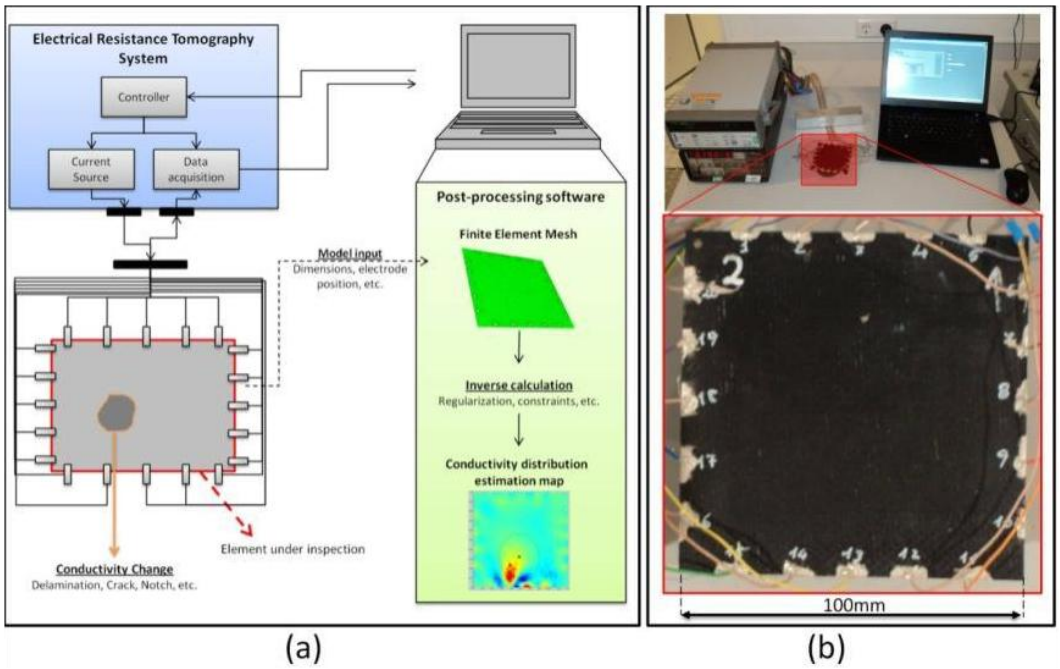

Figure 4. Electrical Resistance Tomography: (a) Conceptual diagram and (b) Developed ERT setup.

4. Results and Discussions

4.1. Properties of the composite and observation of the percolated CNT network

Figure 5 shows a series of SEM pictures at different magnifications. A large number of images was captured at random locations of the composite to verify the homogeneous dispersion of CNT. In Figure 5-a, a macroscopic image of the fracture surface of the composite is seen where the imprints of detached fibers are evident. The fractured surface of the resin reveals the internal distribution of the CNT. A close view of the fracture surface and the fiber-matrix interface is seen in Figure 5–b, c. Individual and clustered CNT are evidently spread in the matrix and are identifiable by their white color in contrast to the darker area of the pure resin. Agglomerated CNT are indicated by ellipses. A better dispersion is evident in Figure 5-c, where a whole region of the resin is covered by randomly dispersed CNT. CNT are present in the inter-fiber region indicating a good infiltration within the layers of glass fibers. Figure 5-d shows a close up of an agglomerate broken at the surface and CNT

protruding from the matrix in a random fashion. The SEM micrographs indicate a high degree of dispersion of the CNT despite the fact that agglomerates are present. This observation in turn gives rise to the presence of a percolated CNT network throughout the composite.

To further verify the percolation of CNT network within the composite, the electrical conductivity of the material in the X, Y and Z directions was experimentally derived. The obtained values were: σ_X = $6.0 \cdot 10^{-3}$ S/m, $\sigma_Y = 6.6 \cdot 10^{-3}$ S/m and $\sigma_Z = 1.5 \cdot 10^{-4}$ S/m. It is seen that the conductivity in the X-Y plane is essentially the same while the value for the Z direction is relatively lower. The difference is not considered significant as all conductivity values achieved fall at the same range as in the works of [3, 8, 29]. Achieving a perfectly dispersed system of CNT is extremely difficult and the intermediate processing steps (layup, curing etc.) play their role in not supporting this. Nevertheless matter-of-factly, this may not be an issue as the achieved 3D network of CNT provides conductive pathways adequate for sensing load, strain and damage [3, 8].

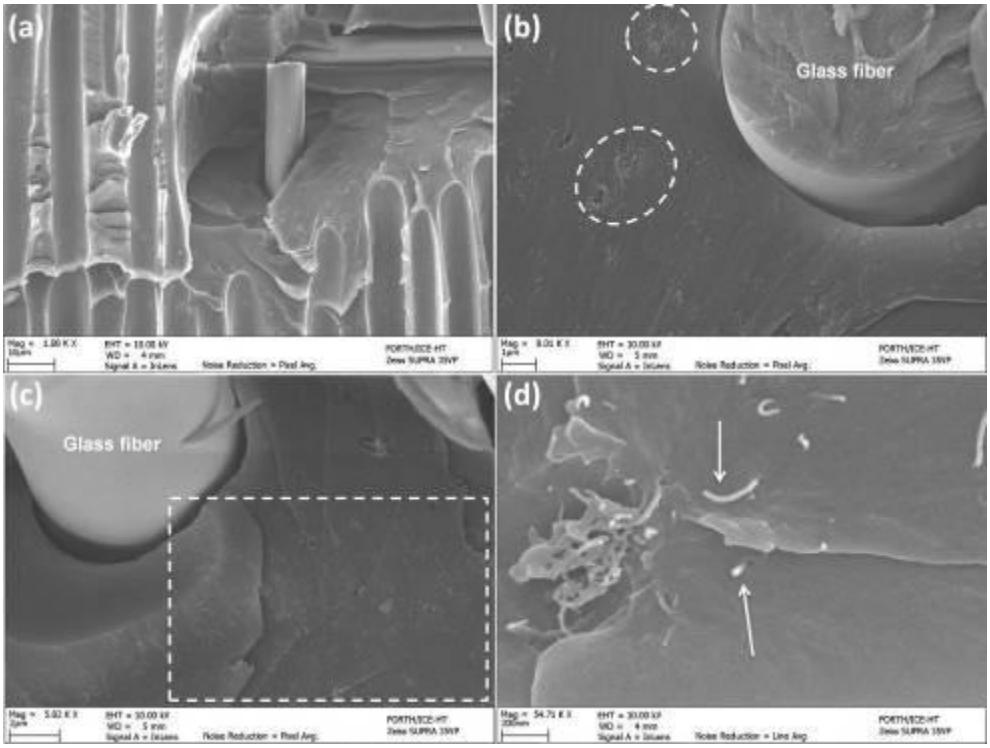

Figure 5. SEM micrographs at different magnifications.

4.2. Sensing Baseline Damage and Cracks

A very small current ($I=10^{-5}$A) was required to reach a signal-to-noise ratio over 50dB for the voltage measurements. This current can produce significant and measurable voltages to enable the detection of changes and, as will be shown later, it was sufficient to distinguish changes between the reference and the damaged state.

The first damage case was used for the baseline evaluation of the approach. A through thickness hole was drilled at (X_{HOLE}, Y_{HOLE}) = (0.0380, 0.0234)m. The damaged specimen is seen in Figure 6-a. Using the recorded values, a conductivity change map is calculated and shown in Figure 6-b. The map shows a smooth baseline in the largest portion of the inspected area. According to the inverse calculation, conductivity change is expected at the central bottom region of the part; close to electrodes 13 and 14. A dipole-like field is predicted close to electrode 13, having similarities to the observations by Proper et al [17], where a distributed mesh of sensors was used. No other region presents specific peaks or other interesting features for further evaluation. From the automated process, the CoI was calculated to be at $(X_{COI\text{-}HOLE}, Y_{COI\text{-}HOLE})$ = (0.0459, 0.0307)m. The respective RoI represents a 16.9% of the total inspected area. Evidently, the hole falls within the identified RoI. Considering the distance between

the real location, the estimated CoI and the size of the inspected area, the localization error is nearly 10% for exactly locating the point of damage. Given this, it can be said that the proposed synergistic NDE approach performs satisfactorily and with marginal error.

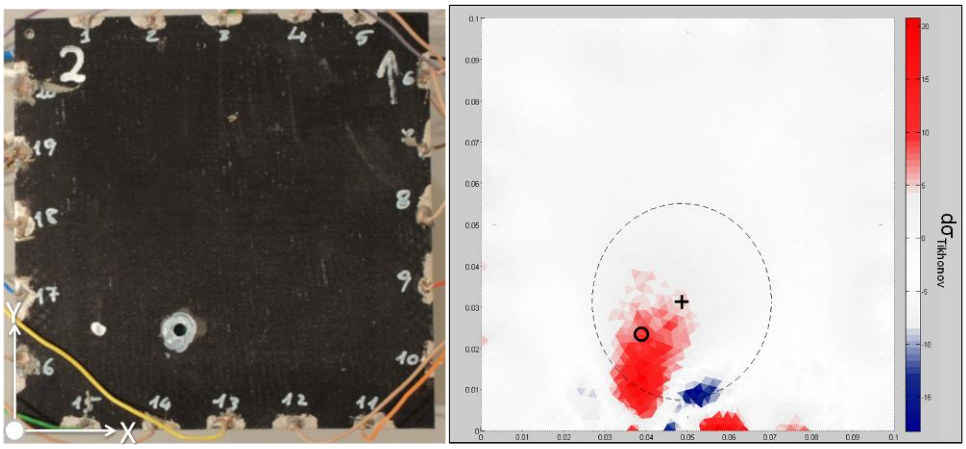

Figure 6. (a) Damaged specimen, (b) Reconstructed conductivity change map; Circle (o) indicates the real damage location, Cross (+) indicates the Centre of Interest, Dashed Ellipse indicates the Region of Interest.

The second damage mode that was assessed was an oblong notch. The notch was created having a -30^o angle to the horizontal. The centre of the notch was at (X_{NOTCH},Y_{NOTCH}) = (0.0630, 0.0705)m. The thickness of the notch was 2mm while the length of the notch was 16mm. The damaged specimen is seen in Figure 7-a. The inserted photograph shows the zoomed region of the notch. The conductivity change map calculated for this damage mode is shown in Figure 7-b. The map is smooth throughout the central region of the inspected area, indicating no changes. An extended region of conductivity change is predicted at the central top region of the part close to electrodes 3 and 4. The CoI for the case of the notch is located at ($X_{COI\text{-}NOTCH}$,$Y_{COI\text{-}NOTCH}$) = (0.0572, 0.0600)m. The RoI represents 22.1% of the total inspected area. Despite the fact that a clear oblong shape change that would directly reflect the notch is not revealed, the notch falls within the identified RoI and close to the CoI with a localization error of nearly 12%.

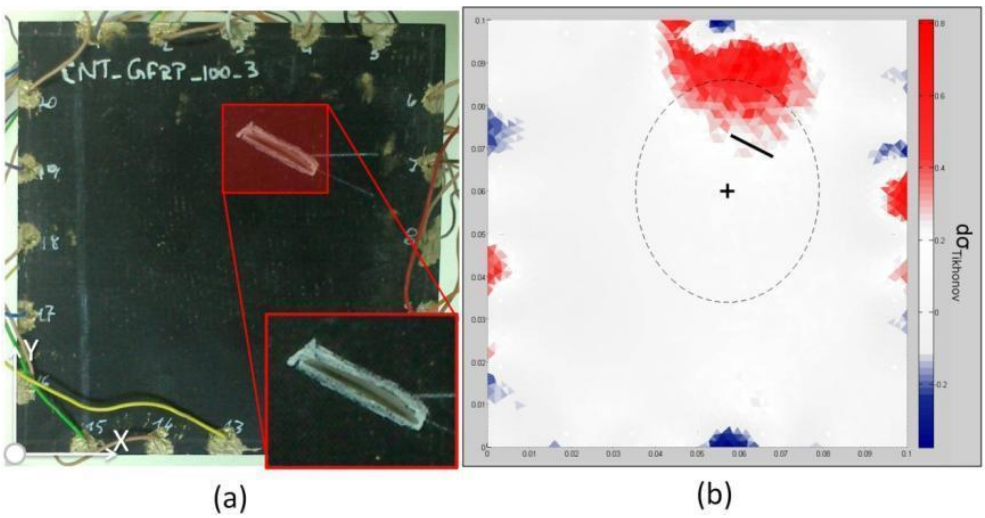

Figure 7. (a) Damaged specimen, (b) Reconstructed conductivity change map; Line indicates the real damage location, Cross (+) indicates the Centre of Interest, Dashed Ellipse indicates the Region of Interest.

As seen from the reconstructed maps, the solution suffers limited resolution away from the electrodes. This is well known in ERT and is due to the ill-posed nature of the problem and the exponential decay of the electric field. In the studied case, this is expressed by low resolution and limited diffusion of the solution in the central region of the part. To improve the situation the optimization of the injection pattern for given expected damage mode and increasing the number of electrodes with respect to the

dimensions of the inspected part could be considered. Current injection strategies that can deliver higher current densities close to the damaged region are required to enhance the sensitivity of the technique. Nevertheless there are certain limitations on what can be expected given the ill-posed nature of ERT. Increasing the number of electrodes may be useful as a means to increase the available information of the developed potential field.

4.3. Quasi-Static Indentation Damage

Figure 8-a shows a snapshot of the QSI experiment. The indentation point was at an off-centre position (X_{QSI}, Y_{QSI}) = (0.0550, 0.0275)m. The corresponding force-displacement curve recorded is shown in Figure 8-b. The experiment was terminated when a drop of the load was recorded which indicated the loss of load bearing capability. The specimen after the indentation is shown in Figure 8-c. The visual inspection revealed a permanent imprint on the indentation side and the debonding of some fiber bundles on the back of the specimen. The corresponding C-scan inspection map is shown in Figure 8-d. According to the benchmark technique, a concentrated change in thickness at the indentation point is revealed as a darker circular region, corresponding to the imprint of the indenter. The local debonding of the bundles just below the indentation point is revealed as dark lines extending in the Y-axis up till after the middle of the specimen. The C-scan shows that the delamination has not propagated in the XY plane. The rest of the part remained intact.

The debonded bundles are impregnated with the resin and thus carry CNT. The fact that the bundles have been detached means that the conductive network at the region has been disrupted and the CNT network around the fibers has been disconnected. Locally, resistance will be larger as the cross-section decreases and this is expected to be reflected on the electrical measurements close to the neighboring electrodes.

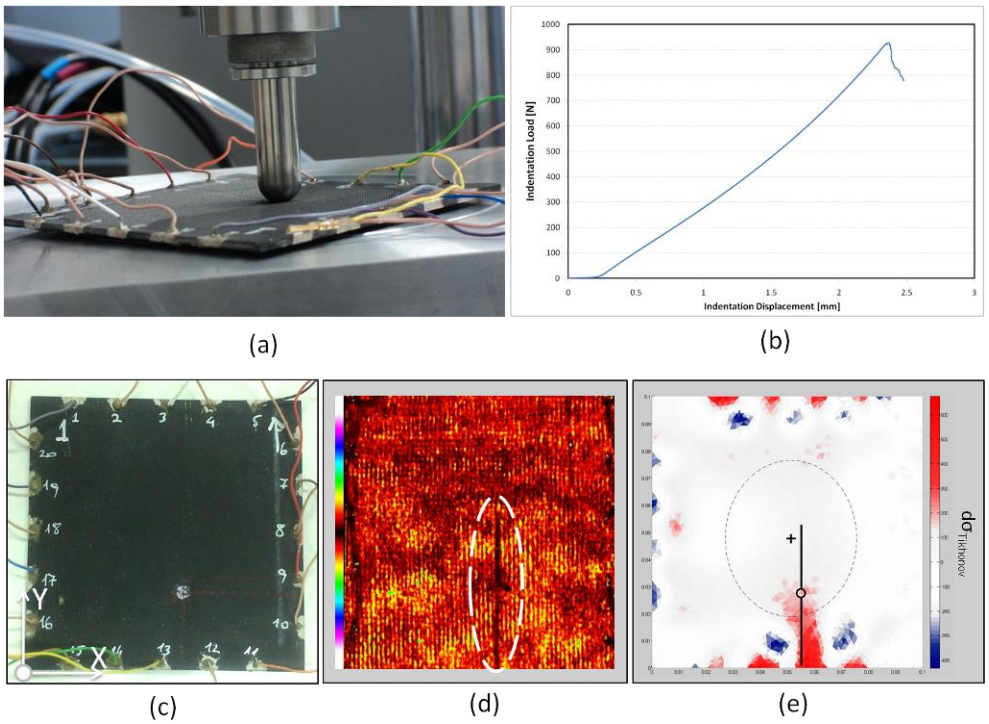

Figure 8. Interlaminar damage mode: (a) snapshot of the indentation experiment, (b) Force displacement diagram recorded for the CNT-GFRP. (c) Damaged specimen (d) Ultrasonic C-scan map, (e) Reconstructed conductivity change map; Circle (o) and continuous lines indicates the real damage location and extend, Cross (+) indicates the Centre of Interest, Dashed Ellipse indicates the Region of Interest.

The experimental voltage recordings before and after the indentation were used to calculate the conductivity change map which is shown in Figure 8-e. The main interesting section of the conductivity change map is at the central bottom region of the part. An oblong strip of conductivity

change is predicted between electrodes 12 and 13 extending up to 1/3 of the plate's Y-dimension. This region corresponds precisely to the real location of the imprint and the fiber bundle debonding. The rest of the map is relatively smooth throughout the central region of the inspected area and some minor pair-wise changes are predicted at the periphery of the part (top and left side).

The CoI for the case of the notch is located at ($X_{COI\text{-}QSI}$, $Y_{COI\text{-}QSI}$) = (0.0513, 0.0476)m. The RoI represents a 25.1% of the total inspected area. Due to the extended dimensions of the real damage, the damage localization error in this case is relatively larger (nearly 18%) than in the other cases. Nevertheless, the largest part of the damaged region, including the indentation point, falls within the identified RoI. Furthermore, the conductivity change region identified correlates with the imprint and the debonding area.

4. Conclusions

The formation of CNT networks within the matrix of an insulating composite using processing techniques compatible with composite manufacturing cycles has offered a new functionality to the structural material (i.e. electrical). Techniques compatible with widely used composite manufacturing techniques are employed to develop the CNT network within composite and exploit it to locate damage in the structural composite. The major conclusions of the work are summarized here:

1. A novel approach based on ERT has been proposed and studied to exploit the created CNT networks within the matrix of the composites for NDE. A structured ERT methodology is presented and applied on CNT reinforced GFRP. Parameters for adapting and customizing the methodology are also discussed.
2. Using ERT procedures it is possible to detect different types of damage that disrupt the structure of the CNT network and are relevant to composites by monitoring disturbances of the electric potential field at the edges of the composite.
3. Electric potential methods for sensing damage in CNT networks are sensitive to very small changes in the network, even as small as 0.1% of the total inspected area. The changes induces in the field by the damage are measureable and convey sufficient information for the ETIP.
4. It is possible to calculate meaningful ETIP solutions based on the proposed formulation. The calculated electrical conductivity change maps of the structure convey meaningful information and can serve well as inspection maps to direct to the location of the damage.
5. The calculated features (i.e. CoI and RoI) performed well in indicating the position of the real damage and successfully predicted the region of it. The inspection area in all the cases was suppressed, reaching up to 83% decrease.

Acknowledgements

Part of this work has been funded by the Seventh Framework Program of the European Commission under the grant agreement No.234333 (project IAPETUS) and No.265593 (project ELECTRICAL). Athanasios Baltopoulos would like to acknowledge the support from the Greek State Scholarship Foundation (IKY), the Greek General Secretariat of Research and Technology and the European Space Agency – Greek Task Force through the ESA Greek Trainee Program.

References

[1] Qiu et al. Carbon nanotube integrated multifunctional multiscale composites. Nanotechnology 2007;18:275708.
[2] Tang et al. Interlaminar fracture toughness and CAI strength of fibre-reinforced composites with nanoparticles – A review. Composites Science and Technology 86 (2013) 26–37
[3] Wichmann et al. Direction sensitive bending sensors based on multi-wall carbon nanotube/epoxy nanocomposites. Nanotechnology 2008;19;475503.
[4] Baltopoulos et al. Sensing strain and damage in polyurethane/MWCNT nano-composite foams using electrical measurements. eXPRESS Polymer Letters 2013;7(1):40–54.

[5] Thostenson et al. Carbon Nanotube Networks: Sensing of Distributed Strain and Damage for Life Prediction and Self Healing. Adv. Mater. 2006;18:2837–2841.
[6] Sotiriadis et al. Stiffness degradation monitoring of carbon nanotube doped glass / vinylester composites via resistance measurements. J Nanostructured Polymers and Nanocomposites 2007;3(03):90-95
[7] Gao et al. In situ sensing of impact damage in epoxy/glass fiber composites using percolating carbon nanotube networks. Carbon 2011;49:3371–3391.
[8] Nofar et al. Failure detection and monitoring in polymer matrix composites subjected to static and dynamic loads using carbon nanotube networks. Comp Sci Technol 2009;69:1599–1606.
[9] Vavouliotis et al. On the fatigue life prediction of CFRP laminates using the Electrical Resistance Change method. Comp Sci Technol 2011;71(5):630-642.
[10] Li et al. Modeling of damage sensing in fiber composites using carbon nanotube networks. Comp Sci Technol 2008;68:3373–3379.
[11] Schueler R, Joshi SP, Schulte K. Damage detection in CFRP by electrical conductivity mapping. Compos Sci Technol 2001;61:921–30.
[12] Angelidis et al. Detection of impact damage in CFRP laminates by means of electrical potential techniques. Comp Sci Technol 2007;67:594–604.
[13] Takahashi et al. Towards practical application of electrical resistance change measurement for damage monitoring using an addressable conducting network. Structural Health Monitoring 2012;11(3):367–377.
[14] Wang et al. Sensitivity of the two-dimensional electric potential/resistance method for damage monitoring in carbon fiber polymer-matrix composite. J Mater Sci 2006; 41:4839–4846.
[15] Lemoine et al. An Electric Potential-based Structural Health Monitoring Technique Using Neural Networks, Proceedings of the 4th International Workshop on Structural Health Monitoring. Stanford, CA, USA, 15-17 September 2003.
[16] Ye et al. Interlaminar fracture and impact damage assessment by electrical resistivity tomography in GFRP laminates with conductive nanoparticles. Proceedings of the 15th European Conference on Composite Materials, Venice, Italy, 24-28 June 2012.
[17] Proper et al. In-Situ Detection of Impact Damage in Composites Using Carbon Nanotube Sensor Networks. Nanoscience and Nanotechnology Letters 2009;1: 3–7.
[18] Hou et al. Spatial conductivity mapping of carbon nanotube composite thin films by electrical impedance tomography for sensing applications. Nanotechnology 2007;18:315501.
[19] Wicks et al. Health Monitoring or Carbon NanoTube (CNT) Hybrid Advanced Composite for Space Applications. Proceedings of the 11th European Conference on Spacecraft Structures, Materials and Mechanical Testing, Toulouse, France, September 2009.
[20] Guzman de Villoria et al. Multi-physics damage sensing in nano-engineered structural composites. Nanotechnology 2011;22:185502.
[21] Baltopoulos et al. Damage identification in CFRP plates using electrical resistance tomography mapping. J Comp Mater, DOI: 10.1177/0021998312464079.
[22] Lionheart et al. The reconstruction problem, in "Electrical Impedance Tomography: Methods, History and Applications", edited by D. Holder, IOP Publishing, Bristol, 2005:3-64.
[23] Vauhkonen et al. Tikhonov Regularization and Prior Information in Electrical Impedance Tomography, IEEE Trans Med Imag 1998;17(2):285-293.
[24] Lazarovitch R, Rittel D, Bucher I. Experimental crack identification using electrical impedance tomography. NDT&E International 2002;35:301-316.
[25] Vavouliotis et al. DC and AC conductivity in epoxy resin/multiwall carbon nanotubes percolative system. Polymer Composites 2010;31:1874–1880.
[26] Athanasopoulos et al. Prediction and experimental validation of the electrical conductivity of dry carbon fiber unidirectional layers. Composites: Part B 42 (2011) 1578–1587
[27] Karhunen et al. Electrical Resistance Tomography imaging of concrete. Cement and Concrete Research 2010;40:137–145.
[28] Polydorides et al. A Matlab toolkit for three-dimensional electrical impedance tomography: a contribution to the Electrical Impedance and Diffuse Optical Reconstruction Software project. Meas Sci Technol 2002;13:1871–1883.
[29] Zhang et al. In situ health monitoring and repair in composites using carbon nanotube additives. Appl Phys Lett 2007;91(13):1–3.